# Effects of Droplet Diameter on the Leidenfrost Temperature of Laser Processed Multiscale Structured Surfaces

Anton Hassebrook[1], Corey Kruse[1], Chris Wilson[2], Troy Anderson[2], Craig Zuhlke[2],
Dennis Alexander[2], George Gogos[1], Sidy Ndao[*1]
University of Nebraska-Lincoln,
[1]Mechanical and Materials Engineering
[2]Electrical Engineering
Lincoln, Nebraska, U.S., 68588
Email: sndao2@unl.edu

## ABSTRACT

In this paper, an experimental investigation of the effects of droplet diameters on the Leidenfrost temperature and its shifts has been carried out. Tests were conducted on a 304 stainless steel polished surface and a stainless steel surface which was processed by a femtosecond laser to form Above Surface Growth (ASG) nano/microstructures. To determine the Leidenfrost temperatures, the droplet lifetime method was employed for both the polished and processed surfaces. A precision dropper was used to vary the size of droplets from 1.5 to 4 millimeters. The Leidenfrost temperature was shown to display shifts as high as 85 $^O$C on the processed surface over the range of droplet sizes, as opposed to a 45 $^O$C shift on the polished surface. The difference between the shifts was attributed to the nature of the force balance between dynamic pressure of droplets and vapor pressure of the insulating vapor layer.

## INTRODUCTION

The Leidenfrost temperature designates the point of minimum heat transfer of a droplet on a hot surface due to the formation of a vapor film, insulator, between the surface and the liquid droplet. Because the Leidenfrost temperature marks the maximum temperature for efficient (nucleate boiling) heat transfer, it is desirable to be able to control and manipulate the Leidenfrost point of a surface. It has been shown in the literature that surface properties such as wettability and roughness as well as fluid properties such as Weber number can have significant effects on Leidenfrost temperature. Recent work carried out by our group demonstrated extraordinary shifts of the Leidenfrost temperature from laser fabricated metallic multiscale Micro/Nanostructured surfaces. The Leidenfrost phenomenon on polished surfaces has been extensively investigated. In general, the Leidenfrost state has been found to be governed by surface chemical properties such as surface energy and composition; thermo-physical properties such as density and thermal conductivity; and also topographic characteristics of the surface the liquid is in contact with (liquid/solid interface). Many studies have shown the Leidenfrost point (LFP) for water on polished stainless steel to be between 280 and 320 $^O$C [1]–[7]; such results have been summarized by Bernardin and Mudawar [7]. Additionally, it has been shown that manipulating surface roughness and nanoporosity can lead to increased wettability, which in turn will increase the LFP [8]–[15].

A more recent publication by Kruse et al. [16], details large shifts in the Leidenfrost temperature on stainless steel via enhanced micro/nanoscale surface roughness. Using Femtosecond Laser Surface Processing (FLSP) techniques to produce superhydrophillic stainless steel surfaces, the LFP was increased from 280 to 455 $^O$C. While others have used coatings, or applied external materials to a surface to change the surface features, our approach does not require the addition of any outside materials.

As evident from the literature cited, extensive research has been performed in regards to determining the Leidenfrost temperature on various surfaces. However, the majority of this work has focused on surface modification techniques while ignoring the contribution of droplet characteristics such as drop volume or diameter. Tamura and Tanasawa [1] have shown the LFP to be seemingly independent of droplet diameter when measured via droplet lifetime. Bernardin et al. [17] have also concluded droplet Weber number to be a nonfactor for droplet impinging a hot surface. In order to develop a more complete understanding of the forces at work on a Leidenfrost droplet on a surface processed via FLSP, further experimentation is necessary. The goal of the present work is therefore to investigate the effects of droplet diameter on the LFP for both a stainless steel surface processed via FLSP and a polished finish.

## EXPERIMENTAL PROCEDURE
### Micro/Nanoscale structure fabrication

In order to fabricate surfaces with tailored wettability, modification of the surface geometry through FLSP is used. A superhydrophillic surface can be created via modification of the surface profile of the steel by generating microscale structures covered with nanoscale particles. No external coatings or materials were applied to the steel surface to obtain the desired structures; the femtosecond laser pulses directly induced modification of the surface. The generation of these surface features is achieved through multi-pulse illumination of the sample with laser fluence above the laser ablation threshold.

Mound structures were produced through the combination of two processing techniques. The first utilizes the square flat topped beam for repetitive stationary laser ablation and fluid flow due to surface melt and tension gradients [18]–[20]. This causes structures to grow until they become large enough to scatter light from incoming laser pulses. This scattering results in larger deposition of laser energy in the valleys than on the structure growths. As this progresses, laser energy causes

preferential valley ablation, induced fluid flow up the sides of the structures, and redeposition of ablated material from the valleys on the tops of the structures [21]–[24]. The second technique is rastering of the Gaussian-shaped beam profile across the sample surface [20]. By varying the laser fluence and number of incident pulses, physical characteristics of surfaces structures can be optimized for spacing, peak to valley height, or structure density, etc. For this project, the test sample was processed with a laser fluence of 1.4 J/cm$^2$ and set to move at a speed such that the number of incident pulses per spot was 1462.

The laser used to produce the test sample was a Spectra Physics Spitfire, Ti:Sapphire femtosecond laser system (Figure 1), which was capable of producing 1 mJ, 50 fs pulses, with a center wavelength of 800 nm. The pulse length and chirp were monitored using a Frequency Resolved Optical Gating (FROG) instrument from Positive Light (Model 8-02).The position of the sample with respect to the laser focal volume was controlled using computer-guided Melles Griot nanomotion translation stages with 3 axes of motion. The laser power was controlled using a half waveplate and a polarizer. All surface processing was completed in open atmosphere [20]. Material composition analysis of the processed sample revealed traces of oxygen which have been attributed to surface oxidation. It should be noted however that the study found no foreign materials (materials not native to the substrate) in the nanoparticle layer [25].
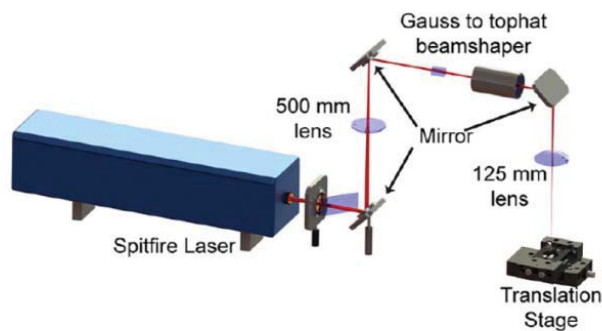


Fig 1. Femtosecond laser setup.

A square-shaped flat-top beam profile with 150 μm sides was used in order to maintain uniform laser fluence on the material surface. This beam profile was created using a refractive beam shaper from Eksma Optics (GTH-4-2.2FA). The laser fluence varied by less than 20% across the central portion of the beam; any fluence fluctuations in the flat-top distribution are attributed to the asymmetries and inhomogeneity of the input beam [20]. Figure 1 shows a schematic diagram of the femtosecond laser setup.

## Leidenfrost Determination

The method used to determine the Leidenfrost point is the droplet evaporation method. This method consists of a droplet being placed on a hot surface while the evaporation time is recorded and plotted as a function of surface temperature. The Leidenfrost point is then defined as the temperature corresponding to the highest evaporation time. For each droplet size and surface temperature, an average of ten droplet lifetimes was taken.

Tests were conducted on two different 304 stainless steel samples, each 64 mm in diameter and 15 mm in thickness. The first sample was polished to a mirror finish by first sanding its surface with 400 grit sandpaper and then polishing it with a buffing compound. The second sample was processed via FLSP. Because a droplet in the Leidenfrost state tends to move around on the surface in a nearly frictionless manner, a conical depression was machined with a 1° slope and a depth of 0.4 mm at the center of the test surface in order to keep the droplet from rolling off the test area. The test surface was heated through the use of cartridge heaters implanted inside a heating block. The heating block, made from copper, had dimensions of 76 mm in diameter and 100 mm in length. The heating block was heated by three equally spaced cartridge heaters. The cartridge heaters used were 0.375 inches in diameter and 3.5 inches in length and were controlled by a programmable Rame-Hart temperature controller with a resolution of 0.1 $^0$C. A standard K-type thermocouple was embedded 0.8 mm below the lowest point on the surface of the samples to provide feedback to the temperature controller. The controller maintained a near constant surface temperature by varying power output to the cartridge heaters.

To ensure consistent droplet sizes, a Rame-Hart precision droplet dispensing unit was used (Figure 2). Drop sizes studied were nominally 1.77, 8.18, and 33.5 μL. These volumes correspond to diameters of 1.5, 2.5, and 4.0 mm respectively. Room temperature droplets (about 20 $^O$C) were released about 2 mm above the test surfaces. To maintain an equal, ambient starting temperature the dropper needle was moved away from the test surface while not in use. At surface temperatures just below or above the LFP, the formation of satellites or smaller droplets due to splitting and splashing from the original droplet became common upon droplet impact. Only full droplets that did not have significant formation of satellites were considered for measurements.

## RESULTS AND DISCUSSION

Figure 4 shows the SEM images and 3D profilometry scans of the processed and polished surfaces used in the Leidenfrost experiments. Characterization of both surfaces was carried out using Scanning Electron Microscope and a Keyence VK-X200 3D confocal laser scanning microscope. As can be seen from the figure, the processed surface consists of self-assembled microsctructures characterized by deep holes separating pointed structures also known as Above Surface Growth Mounds (ASG-Mounds). From the 3D confocal laser scanning microscope data, surface roughness and microstructures height information could be obtained: microstructures on the processed surface had an average height of 18.4 μm and a maximum height of 31.8 μm with a surface roughness $R_{rms}$ value of 4.8 μm while the polished surface had a measured $R_{rms}$ value of 0.04 μm.
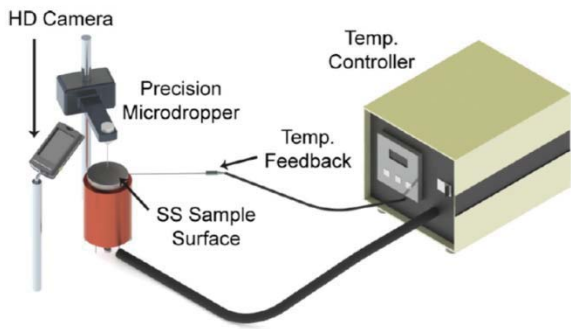
Fig 2. Leidenfrost setup.

Contact angle measurements were also carried out using a Rame-Hart Model 590 F4 series Goniometer and Tensiometer. All contact angle measurements were done with 1 μL droplets of ASTM Type II deionized water. Contact angle measurements were taken at a variety of random locations on each surface; and contact angle results were found to be independent of droplet location. Contact angles on the processed surface were found to be equal to 0 $^O$C while the polished sample had an equilibrium contact angle of 75 $^O$C. Contact angle measurements were repeated on a weekly basis throughout the duration of testing for both samples. Because the samples were stored in open air, oxidation and carbon build up caused changes in wettability over time. Over a time period of a few weeks, the contact angles were found to decrease for the polished sample, and increase for the processed sample. However a 20 minute ultrasonic bath in isopropyl alcohol would completely restore the wettability properties of the samples. In addition to ultrasonic bath, the surface of polished sample was often wiped with a Clorox wipe.

Figure 4 shows the results of the Leidenfrost experiments. The error bars represent the standard deviation of 10 data points for each surface temperature. It should be noted that the error bars tend to be small (around 5% of total lifetime) at temperatures far above the LFP. As surface temperature decreases, the error bars increase to about 10% of total lifetime around the LFP. As indicated on the figure, The LFP is defined as the temperature corresponding to the highest evaporation time. Date point to the left and right of the LFP correspond to droplets in transition and film boiling regimes respectively. Overall the LFP on the processed surface is higher than that of the polished surface for all droplet sizes investigated. More on the effects of microstructures and contact angle on the LFP can be found on a recently published paper by our group [16]. As for the effects of droplet size, the LFP was shown to shift 45 $^O$C over the range of droplet sizes on the polished sample compared to 85 $^O$C over the same range of droplet sizes on the ASG-Mounds sample. With the smallest droplet size, 1.5 mm, there is a difference of 140 $^O$C between the LFP of the two samples as seen on Figure 5. This difference shifted to 200 $^O$C at the largest droplet diameter of 4.0 mm. This trend shows that not only does the Leidenfrost temperature increases with droplet diameter but also the rate at which it increases varies from the polished sample to the processed sample. This indicates that the presence of
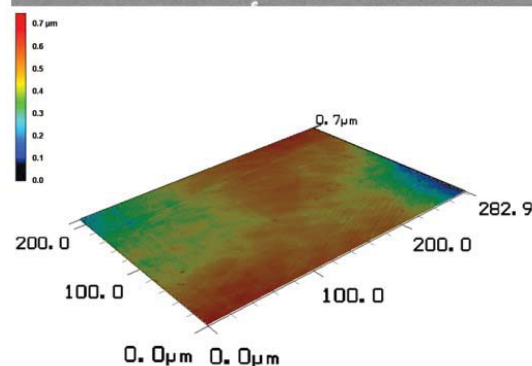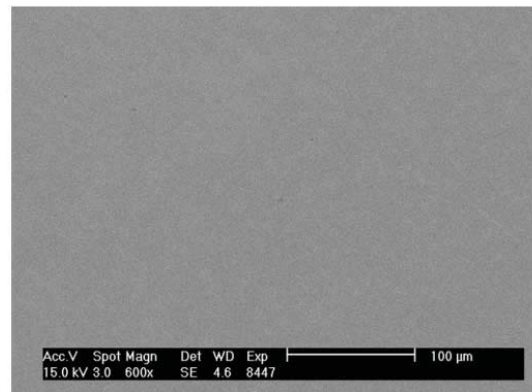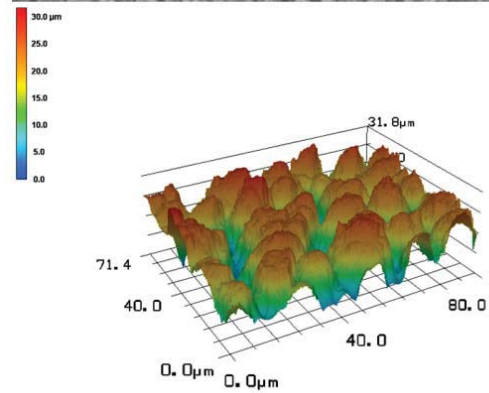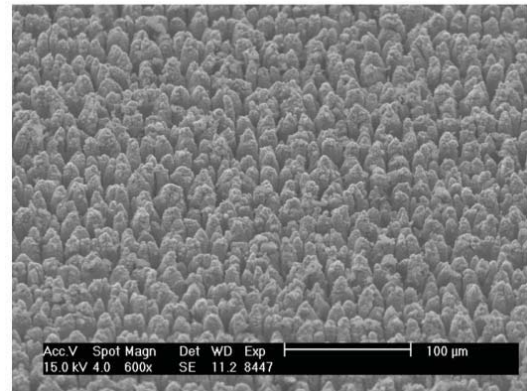


Fig 3. SEM images and 3D topology scans of ASG-Mounds (top) and mirror polished (bottom) test samples. SEM images taken at 600x magnification – scale bars are 100 microns. It should be noted that the colors do not correspond on the topology scans. For the ASG-Mounds red represents a height of 30 microns, while the same color represents a height of 0.7 microns on the polished sample.
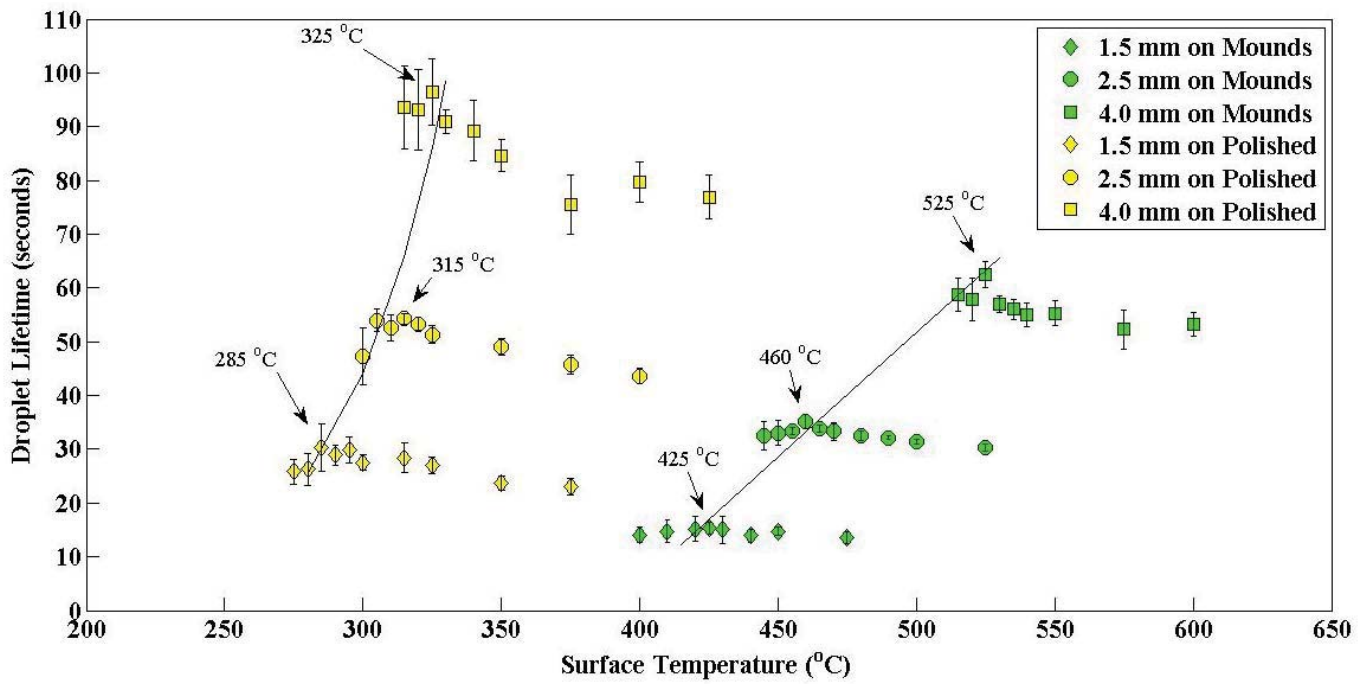
Fig 4. Droplet lifetime curves of water droplets on polished (yellow) and FLSP (green) stainless steel test surfaces.
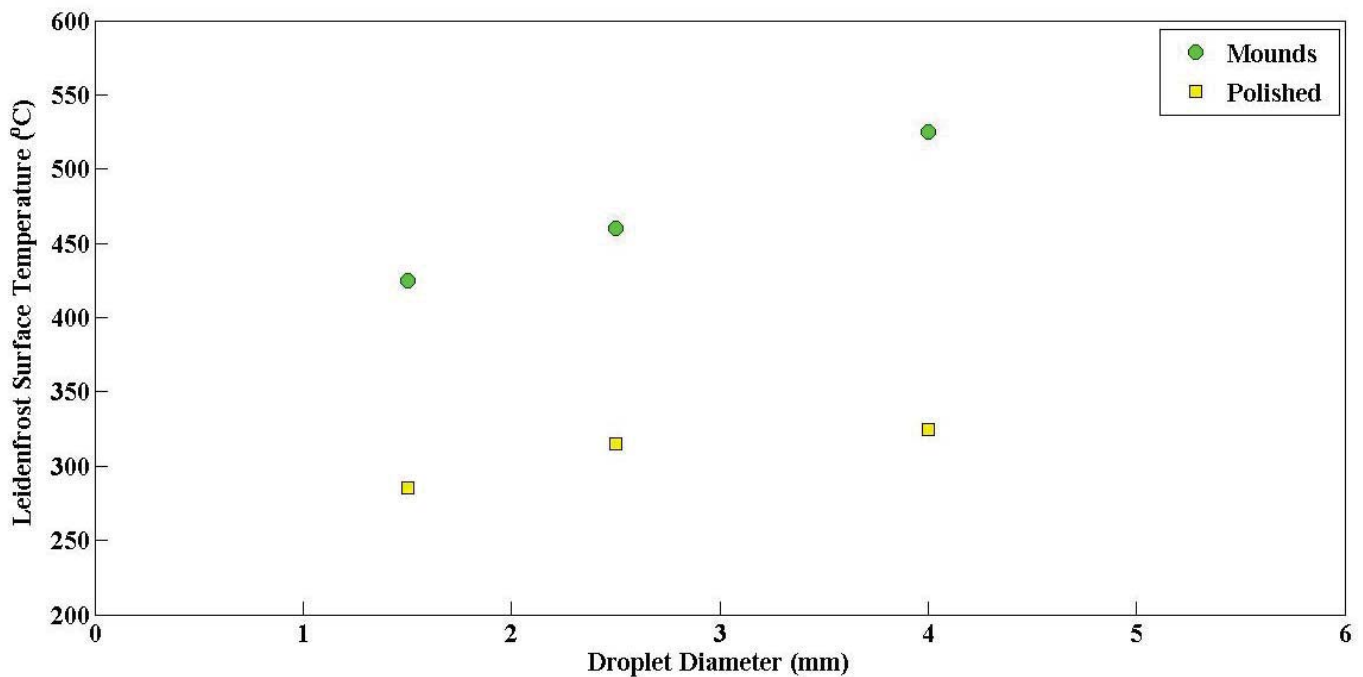


Fig 5. Discrete Leidenfrost points from the lifetime curves shown with respect to diameter.

microstructures on the processed surface adds a new mechanism to the diameter-dependent LFP, a mechanism which has been discussed in the open literature yet.

What follows is a hypothesis in an attempt to explain the observed results. When vapor is formed beneath the droplet, it must escape as a result of conservation of mass. In the case of the polished sample, the vapor escapes radially outward away from the droplet center. This flow profile creates a pressure field below the droplet which in turn produces a net upward force on the droplet, hence the levitation. This net upward force is applied to the projected area of the droplet and balances the weight of the droplet. As the droplet size is increased or decreased, both the droplet shape and the vapor layer thickness change as well [26], [27]. For large droplets, the shape of the droplet takes on a pancake profile while small

droplets are more spherical. Also, the vapor layer thickness increases with droplet size. As the droplet size increases, the projected area of the droplet also increases. The vapor layer thickness and projected area are two contrasting parameters. As the projected area increases, it takes less force to balance the droplet but as the vapor layer thickness increases there is less flow restriction and less pressure beneath the droplet. An area ratio can be formed between the projected area and the radial perimeter area that the vapor escapes through. This ratio is thought to vary with the changing droplet size but not significantly because the two parameters both increase with droplet size. The weight of the droplet however significantly changes with droplet size. This is believed to be the major factor in the increase of the Leidenfrost point for the polished sample. If the area ratio is nearly the same for all droplet sizes, the increase in weight is a major factor. As the weight increases the net upward force needed to balance the droplet must also increase. This results in a higher surface temperature and energy which provides the larger force needed.

In the case of the processed sample, everything is the same except the addition of the microstructures. The major shift in the Leidenfrost temperature is mainly due to the reduction in contact angle as well as increased surface roughness. It is expected that the change in the Leidenfrost temperature with respect to the droplet size would be nearly the same for both the polished and processed sample. However as seen in Figure 5, the slopes for the polished and processed surface are not the same. This means that the microstructures play a larger role in shifting the Leidenfrost temperature for large droplets. It is believed that the microstructures play a significant role in changing the area ratio previously described. The microstructures layer is a very rough and porous layer, allowing more area for the generated vapor to escape through. This is essentially artificially increasing the vapor layer thickness. As a result of this, the vapor has a less restrictive flow path and thus produces less pressure beneath the droplet. This means that the droplet requires higher surface temperatures and energy to produce enough upward force to balance the droplet. It is also believed that the microstructures have a more significant effect on the area ratio of larger droplets. This effect is what causes the slope of the curves to be different. This trend may however not hold for fluids having different thermophysical properties than DI water.

## CONCLUSIONS

The effects of droplet size on the Leidenfrost temperature for both polished and processed stainless steel surfaces have been studied. Femtosecond Laser Surface Processing (FLSP) has been used to tailor the surface roughness of a stainless steel test sample via the creation of multiscale micro/nanostructures. These multiscale structures alter the roughness, wettability, and nanoporosity of the surface, which in turn have large effects on the Leidenfrost temperature. These surface effects work in conjunction with the effects of increasing droplet size to produce shifts in the Leidenfrost Point as high as 200 $^{O}$C. The shifts can be attributed to a changing force balance between the weight of a droplet placed on a superheated surface and vapor pressure of the insulating vapor film. In the case of the processed surface, the combination of microstructure spacing and nanoporosity worked alter the pressure field below the droplet, resulting in an additional shift that could not be explained purely by surface characteristics.

## REFERENCES

[1] Z. Tamura and Y. Tanasawa, "Evaporation and Combustion of a Drop Contacting with a Hot Surface," Symp. Combust., vol. 7, pp. 509–522, 1958.

[2] K. Baumeister, R. Henry, and F. Simon, "Role of the Surface in the Measurement of the Leidenfrost Temperature," Augment. Convect. Heat Mass Transf. A. E. Bergles R. L. Webb, eds., ASME, New York, pp. 91–101, 1970.

[3] G. S. Emmerson, "The Effect of Pressure and Surface Material on the Leidenfrost Point of Discrete Drops of Water," Int. J. Heat Mass Transf., vol. 18, no. 3, pp. 381–386, 1975.

[4] T. Y. Xiong and M. C. Yuen, "Evaporation of a Liquid Droplet on a Hot Plate," Int. J. Heat Mass Transf., vol. 34, no. 7, pp. 1881–1894, 1991.

[5] N. Nagai and S. Nishio, "Leidenfrost Temperature on an Extremely Smooth Surface," Exp. Therm. Fluid Sci., vol. 12, no. 3, pp. 373–379, Apr. 1996.

[6] H. Kim, B. Truong, J. Buongiorno, and L.-W. Hu, "On the Effect of Surface Roughness Height, Wettability, and Nanoporosity on Leidenfrost Phenomena," ppl. Phys. Lett., vol. 98, no. 8, p. 083121, 2011.

[7] J. D. Bernardin, "The Leidenfrost Point : Experimental Study and Assessment of Existing Models," vol. 121, no. November, 1999.

[8] I. U. Vakarelski, N. a Patankar, J. O. Marston, D. Y. C. Chan, and S. T. Thoroddsen, "Stabilization of Leidenfrost Vapour Layer by Textured Superhydrophobic Surfaces.," Nature, vol. 489, no. 7415, pp. 274–7, Sep. 2012.

[9] F. Hughes, "The Evaporation of Drops from Super-Heated Nano-Engineered Surfaces," Dr. Diss. Massachusetts Inst. Technol., 2009.

[10] Y. Takata, S. Hidaka, a. Yamashita, and H. Yamamoto, "Evaporation of Water Drop on a Plasma-Irradiated Hydrophilic Surface," Int. J. Heat Fluid Flow, vol. 25, no. 2, pp. 320–328, Apr. 2004.

[11] R. a. Munoz and D. Beving, "Hydrophilic Zeolite Coatings for Improved Heat Transfer," Ind. Eng. Chem. Res., vol. 44, no. 12, pp. 4310–4315, Jun. 2005.

[12] C.-K. Huang and V. P. Carey, "The Effects of Dissolved Salt on the Leidenfrost Transition," Int. J. Heat Mass Transf., vol. 50, no. 1–2, pp. 269–282, Jan. 2007.

[13] D. A. del Cerro, A. G. Marín, G. R. B. E. Römer, B. Pathiraj, D. Lohse, and A. J. Huis in 't Veld, "Leidenfrost Point Reduction on Micropatterned Metallic Surfaces.," Langmuir, vol. 28, pp. 15106–10, 2012.

[14] P. Bizi-Bandoki, S. Benayoun, S. Valette, B. Beaugiraud, and E. Audouard, "Modifications of Roughness and Wettability Properties of Metals Induced by Femtosecond Laser Treatment," Appl. Surf. Sci., vol. 257, no. 12, pp. 5213–5218, Apr. 2011.

[15] Z. K. Wang, H. Y. Zheng, and H. M. Xia, "Femtosecond Laser-Induced Modification of Surface Wettability of PMMA for Fluid Separation in Microchannels," Microfluid. Nanofluidics, vol. 10, no. 1, pp. 225–229, Jul. 2010.

[16] C. Kruse, T. Anderson, C. Wilson, C. Zuhlke, D. Alexander, G. Gogos, and S. Ndao, "Extraordinary Shifts of the Leidenfrost Temperature from Multiscale Micro/nanostructured Surfaces.," Langmuir, vol. 29, no. 31, pp. 9798–806, Aug. 2013.

[17] J. Bernardin, C. Stebbins, and I. Mudawar, "Effects of Surface Roughess on Water Droplet Impact History and Heat Transfer Regimes.pdf." International Journal of Heat and Mass Transfer, pp. 73–88, 1996.

[18] G. D. Tsibidis, M. Barberoglou, P. a. Loukakos, E. Stratakis, and C. Fotakis, "Dynamics of Ripple Formation on Silicon Surfaces by Ultrashort Laser Pulses in Subablation Conditions," Phys. Rev. B, vol. 86, no. 11, p. 115316, Sep. 2012.

[19] A. Y. Vorobyev and C. Guo, "Direct Femtosecond Laser Surface Nano/microstructuring and Its Applications," Laser Photon. Rev., vol. 7, no. 3, pp. 385–407, May 2013.

[20] C. Zuhlke, T. Anderson, and D. Alexander, "Formation of Multiscale Surface Structures on Nickel via above Surface Growth and below Surface Growth Mechanisms Using Femtosecond Laser Pulses," Opt. Express, vol. 21, no. 7, pp. 97–98, 2013.

[21] C. H. Crouch, J. E. Carey, J. M. Warrender, M. J. Aziz, E. Mazur, and F. Y. Génin, "Comparison of Structure and Properties of Femtosecond and Nanosecond Laser-Structured Silicon," Appl. Phys. Lett., vol. 84, no. 11, p. 1850, 2004.

[22] T.-H. Her, R. J. Finlay, C. Wu, and E. Mazur, "Femtosecond Laser-Induced Formation of Spikes on Silicon," Appl. Phys. A Mater. Sci. Process., vol. 70, no. 4, pp. 383–385, Apr. 2000.

[23] F. Sánchez, J. L. Morenza, and V. Trtik, "Characterization of the Progressive Growth of Columns by Excimer Laser Irradiation of Silicon," Appl. Phys. Lett., vol. 75, no. 21, p. 3303, 1999.

[24] B. R. Tull, J. E. Carey, E. Mazur, and S. M. Yalisove, "S Ilicon Surface Morphologies after Femtosecond Laser Irradiation," vol. 31, no. August, pp. 626–633, 2006.

[25] C. a. Zuhlke, T. P. Anderson, and D. R. Alexander, "Comparison of the Structural and Chemical Composition of Two Unique Micro/nanostructures Produced by Femtosecond Laser Interactions on Nickel," Appl. Phys. Lett., vol. 103, no. 12, p. 121603, 2013.

[26] A.-L. Biance, C. Clanet, and D. Quéré, "Leidenfrost Drops," Phys. Fluids, vol. 15, no. 6, p. 1632, 2003.

[27] J. C. Burton, a. L. Sharpe, R. C. a. van der Veen, a. Franco, and S. R. Nagel, "Geometry of the Vapor Layer Under a Leidenfrost Drop," Phys. Rev. Lett., vol. 109, no. 7, p. 074301, Aug. 2012.